Exp. Theo. NANOTECHNOLOGY 10 (2026) 37-46 https://doi.org/10.56053/10.1.37

A fuzzy sliding mode control for a robotic system

Lafi AL NUFAIE[*]

Department of Electrical Engineering, College of Engineering, Shaqra University, Al Dawadmi, 11961, Saudi Arabia
[*]) Email: lalnufaie@su.edu.sa

Received 15/10/2025, *Received in revised form* 28/11/2025, *Accepted* 15/12/2025, *Published* 15/1/2026

Basically, miniaturized versions of robotic arms, micro and even nano robotic arms are the perfect candidate for performing accurate inspections at microscopic scales on structures. With relatively small actuators and sensors, they are ideal for looking for small defects and components.The growing challenges of robotization for a flexible and efficient industry require the development of reliable, precise, and efficient robotic systems. In this context, we propose an approach combining fuzzy logic and sliding modes to obtain robust, simple, and efficient control for a SCARA robot. Simulation results are presented to corroborate our claims.

Keywords: Type-2 fuzzy systems; Sliding mode control; Robotic Systems.

1. INTRODUCTION

Nanorobots are incredibly tiny, controllable machines built at the smallest molecular scale. The science of building them, called nanorobotics, is still new but takes ideas from regular robotics. Scientists are now starting to create these devices, often by copying designs found in nature. Today, their most important use is in medicine and healthcare. we present a comprehensive review of recent nanorobotics-enabled biomedical applications, specifically addressing oncotherapy, cerebral aneurysm intervention, nephrolithiasis ablation/removal, and nanoscale DNA repair, as well as complementary therapeutic modalities that promise substantial reductions in mortality. The review analyzes structural designs, actuation schemes, control algorithms, biosafety and regulatory considerations, and translational pathways. Robotization underpins the capability of future industries and Industry 4.0 factories to meet rising demands and complexity. It can be considered a primary tool for flexible automation, not only by facilitating the accomplishment of repetitive and dangerous tasks, but also by increasing production efficiency and consistency. To attain these objectives, it is necessary to develop controllers that enable

robotic systems to combine speed and precision, which are antagonistic properties. Moreover, this type of system is subject to parametric variations, which makes the model used uncertain, and to external disturbances [1].

To address robustness concerns, sliding mode control has been extensively studied as a classical robust control methodology [1-2]. The main idea is to use two control signals. A discontinuous one drives the system state to a predefined sliding surface. The second signal keeps the system on the sliding surface and drives the states to zero. A well-designed sliding mode controller makes the system insensitive to counter matched disturbances and uncertainties as the state evolves along the sliding surface [3-6]. Nevertheless, the presence of chattering phenomena represents the main drawback of this approach, in addition to the knowledge of the system model. To solve these problems, sliding mode control has been fused with other techniques to create adaptive sliding-mode control [7-10], neural network sliding mode control [11-14], fuzzy sliding mode control [14-16]. A variety of approaches have been reported in the literature, including substituting the signum function with saturation. [18], using a fuzzy system [15-17], or employing a nonlinear sliding surface [18]. Chattering can be mitigated, but finite-time convergence to zero remains unresolved.

In this sense, Terminal sliding mode control can be adopted for the problem of finite-time convergence [18-20]. However, due to the presence of fractional powers and their derivatives, terminal sliding mode control encounters a singularity problem, which prevents it from achieving convergence of tracking errors when the system states reach zero [22]. We developed a nonsingular fast terminal sliding-mode controller, offering the advantages of conventional terminal sliding mode control while significantly improving convergence speed and overcoming the singularity problem [23].

In this work, we introduce a new controller that combines the benefits of nonsingular fast terminal sliding mode control and interval type-2 fuzzy logic for the SCARA robot application. Type-2 fuzzy systems initially identify and estimate the unknown terms. The nonsingular terminal sliding mode control law is formulated to guarantee consistent convergence time and robust performance, and robustness. The type-2 fuzzy systems are updated based on adaptation laws derived from stability analysis. Simulations demonstrate the proposed approach's effectiveness [24-26].

The rest of the paper is organized as follows: Section 2 introduces interval type-2 fuzzy systems. Section 3 describes the dynamic model of a SCARA robot. In Section 4, we discuss the controller design and the stability analysis. Section 5 presents the simulation study and results that demonstrate the effectiveness of the proposed approach. The paper concludes with a final conclusion.

2. MATERIALS AND METHODS

2.1 Interval Type-2 fuzzy logic system

Interval type-2 fuzzy system (IT2FS is the most commonly used version of type-2 fuzzy systems (T2F) due to its simple design and reduced calculation time compared to the general form [18]. To reduce calculation time, we propose using triangular fuzzy sets in this work. An interval type-2 fuzzy set is characterized by its footprint of uncertainty (FOU), the region between the upper and lower membership functions, referred to as the footprint of uncertainty (FOU). $\bar{\mu}_{\tilde{A}(x)}$ and $\underline{\mu}_{\tilde{A}(x)}$. This is the footprint of uncertainty (FOU). Let M be the number of rules in the Type-2 fuzzy rule base, each written as the following form:

$$R^i = \text{IF } x_1 \text{ is } \tilde{F}_1^i \text{ and } \ldots\ldots x_n \text{ is } \tilde{F}_n^i \text{ then } y \text{ is } \left[w_l^i \quad w_r^i\right]$$

where $x_j = 1,2,3,\ldots\ldots,n$ and y are the input and output variables of the interval type-2 fuzzy system (T2FS), respectively, used for modeling, the $\tilde{F}_j^i$ are the type-2 fuzzy sets constituting the antecedent part and $\left[w_l^i \quad w_r^i\right]$ The weighting interval is in the consequent part. Type-reduction converts a type-2 fuzzy

set to a type-1 set. Meanwhile, the firing strengthF_i for the ith rule, an interval type-2 set, can be written as:

$$F^i = \left[\underline{f^i} \quad \overline{f^i}\right]$$

where

$$\underline{f^i} = \underline{\mu}\tilde{F}_1^i(x_1) * \ldots\ldots * \underline{\mu}\tilde{F}_n^i(x_n)$$

$$\overline{f^i} = \underline{\mu}\tilde{F}_1^i(x_1) * \ldots\ldots * \underline{\mu}\tilde{F}_n^i(x_n)$$

Using the center-of-set type-reduction, we obtain the IT2FS output in the vectorized form presented below:

$$y(x) = \Lambda^T(x).\phi \quad (1)$$

where $\Lambda(x)$ represents the regressive vector, and ϕ denotes the consequent vector containing the conclusion values of the fuzzy rules.

2.2 Dynamic model of SCARA robot

Figure 2 represents a simplified structure of a SCARA robot; it has three rotational joints in the plane (X − Y). The three rotational actuators are labeled Shoulder, Elbow, and Wrist, in that order, per Figure 1. The general Newton-Euler Equations for a manipulator can be written in the form:

$$M(\theta)\ddot{\theta} + V(\theta,\dot{\theta})\dot{\theta} + G(\theta) + \tau_f = \tau \quad (2)$$

where $\theta, \dot{\theta}, \ddot{\theta}$ denote the position, velocity and acceleration n×1 vectors, respectively, $M(\theta)$ is the n×n , inertia matrix of the robot, $V(\theta,\dot{\theta})$ is an n×n the centrifugal–Coriolis term matrix, and $G(\theta)$ is an n×1 gravity-term vector, τ_f is the n×1 vector of external disturbances, and the n×1 vector τ_f represents actuator torques. Since we are focused on the three rotational joints, with motion constrained to the X−Y motion, The gravity-term vector reduces to zero as follows:

$$G(\theta) = 0 \quad (3)$$

Expressions of terms of Equation (1) are given in Appendix A. The dynamical model of our system can be rewritten as:

$$\ddot{\theta} = -M^{-1}(\theta)V(\theta,\dot{\theta})\dot{\theta} + M^{-1}(\theta)\tau + M^{-1}(\theta)\tau_f \quad (4)$$

Equation (4) can be reformulated as follows:

$$\ddot{\theta} = F(\theta,\dot{\theta}) + B_o(\theta)\tau + \tau_{dis} \quad (5)$$

where $F(\theta,\dot{\theta}) = -M^{-1}(\theta)V(\theta,\dot{\theta})\dot{\theta}$, $B_0(\theta)$ denotes the nominal well-known value of $M^{-1}(\theta)$, and τ_{dis} regroups all external disturbances and uncertainties.

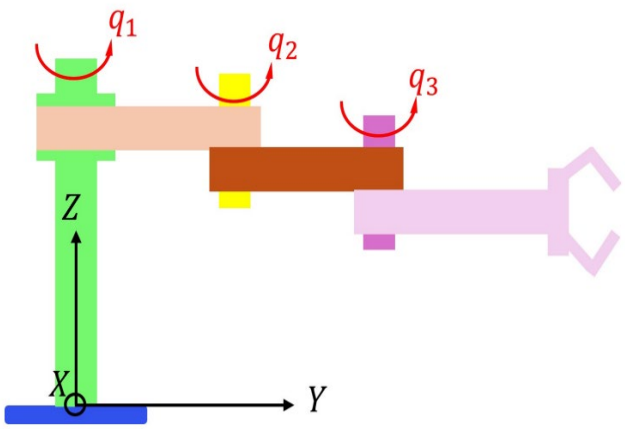

Figure 1 SCARA robot manipulator.

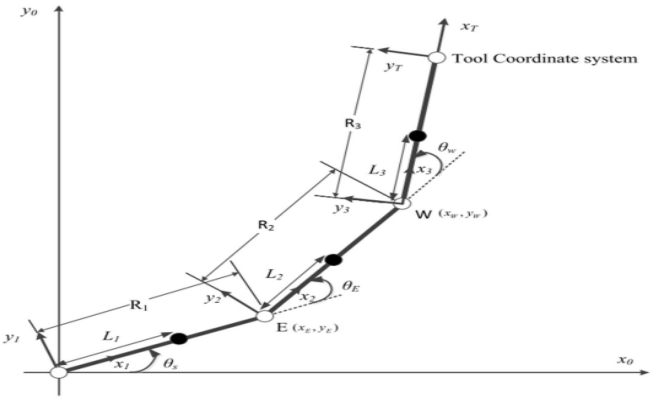

Figure 2 Schematic diagram of the SCARA robot.

As given in [19], the most concise of τ_{dis} can be expressed in Equation (6) as:

$$\tau_{dis} \leq b_0 + b_1|\theta| + b_2|\dot{\theta}|^2 \quad (6)$$

where b_0, b_1 and b_2 are strictly positive scalars.

2.3 Design approach of NST sliding mode control law

In this subsection, this work aims. A robust controller is designed using a nonsingular fast terminal sliding mode (NFTSM) approach to guarantee the desired tracking performance [3,24]. The tracking error is initially defined by:

$$e_1 = \theta_d - \theta$$
$$e_2 = \dot{\theta}_d - \dot{\theta} \quad (7)$$

where $\theta_d, \dot{\theta}_d$, represent the desired trajectory of θ and $\dot{\theta}$ respectively.

Then, the nonsingular terminal sliding can be written as:

$$\sigma(t) = e_1 + k_1|e_1|^{\alpha_1}\text{sign}(e_1) + k_2|e_2|^{\alpha_2}\text{sign}(e_2) \quad (8)$$

where k_1, k_2, α_1 and α_2 are positive scalars, with $1 < \alpha_2 < 2$ and $\alpha_2 < \alpha_1$; $\text{sign}(\cdot)$ designs the signum function defined as:

$$\text{sign}(x) = \begin{cases} 1 & \text{if } x > 0 \\ 0 & \text{if } x = 0 \\ -1 & \text{if } x < 0 \end{cases}$$

From Equation (7), the sliding surface is defined to enforce finite-time convergence to the desired trajectories. When initial conditions are far from the target, convergence speed is governed by the dominant term $k_1|e_1|^{\alpha_1}\text{sign}(e_1)$ Near the target, the term $k_2|e_2|^{\alpha_2}\text{sign}(e_2)$ ensures convergence in finite time [22,27] . As time passes, the sliding surface's derivative becomes:

$$\dot{\sigma}(t) = e_2 + \alpha_1 \cdot k_1|e_1|^{\alpha_1 - 1}e_2 + \alpha_2 \cdot k_2|e_2|^{\alpha_2 - 1} \cdot \dot{e_2} \quad (9)$$

As explained above, the control signal will consist of two terms. The first one, $\tau_s(t)$, the switching signal, denoted as $\tau_s(t)$, has the objective of driving the system back to surface. The second term, $\tau_e(t)$ Equivalent control is employed to sustain the trajectory on the sliding surface. (7). To design $\tau_e(t)$, We assume that the system resides on the sliding surface., $\sigma(t) = 0$, and remains on, $\dot{\sigma}(t) = 0$. Thus, the system is invariant to uncertainties and external disturbances [9]. Using Equations (6) and (8), Equation (9) can be rewritten as:

$$\dot{\sigma}(t) = e_2 + \alpha_1 \cdot k_1|e_1|^{\alpha_1 - 1}e_2 + \alpha_2 \cdot k_2|e_2|^{\alpha_2 - 1} \cdot \dot{\theta}_d - \alpha_2 \cdot k_2|e_2|^{\alpha_2 - 1} \cdot \left[F(\theta, \dot{\theta}) + B_o(\theta)\tau_e\right] \quad (10)$$

Using the fact that $\dot{x} = |\dot{x}| \cdot sign(\dot{x})$ The expression for the equivalent control law is given by:

$$\boldsymbol{\tau_e(t) = B_0^{-1}(\theta)\left[F(\theta,\dot{\theta}) + \ddot{\theta}_d + [\alpha_2 \cdot k_2]^{-1} \cdot |e_2|^{2-\alpha_2}\right] + [\alpha_2 \cdot k_2]^{-1}|e_2|^{2-\alpha_2}(\alpha_1 \cdot k_1|e_1|^{\alpha_1-1})sign(e_2)]} \quad (11)$$

The switching signal expression is derived as follows: $\tau_s(t)$ aimed at ensuring the system reaches the sliding surface under uncertainties and disturbances. Incorporating the disturbance term, Equation (9) becomes: $\tau_{dis}(t)$:

$$\dot{\sigma}(t) = e_2 + \alpha_1 \cdot k_1|e_1|^{\alpha_1-1}e_2 + \alpha_2 \cdot k_2|e_2|^{\alpha_2-1} \cdot \ddot{\theta}_d - \alpha_2 \cdot k_2|e_2|^{\alpha_2-1} \cdot \left[F(\theta,\dot{\theta}) + B_o(\theta)\tau_e + \tau_{dis}\right] \quad (12)$$

Using Equation (11), the time derivative of the sliding surface in Equation (12) may be rewritten as:

$$\dot{\sigma}(t) = e_2 + \alpha_1 \cdot k_1|e_1|^{\alpha_1-1}e_2 + \alpha_2 \cdot k_2|e_2|^{\alpha_2-1} \cdot \ddot{\theta}_d - \alpha_2 \cdot k_2|e_2|^{\alpha_2-1} \cdot [F + B_o(\theta) \cdot (\tau_e + \tau_s) + \tau_{dis}] \quad (13)$$

Applying the definition of equivalent control yields, $\tau_e(t)$ in Equation (11), Equation (13) This can be simplified to:

$$\dot{\sigma}(t) = -\alpha_2 \cdot k_2|e_2|^{\alpha_2-1} \cdot [B_o(\theta) \cdot \tau_s + \tau_{dis}] \quad (14)$$

To deduce the expression of τ_s . This enables us to drive the system to the sliding surface. To analyze stability, consider the following Lyapunov function:

$$V(t) = 0.5\,\sigma^2(t) \quad (15)$$

$V(t)$ in Equation (15), according to time and using Equation (14) leads to:

$$\dot{V}(t) = \sigma(t)[\alpha_2 \cdot k_2|e_2|^{\alpha_2-1} \cdot [B_o(\theta) \cdot \tau_s + \tau_{dis}]] \quad (16)$$

If we choose the switching signal $\tau_s(t)$ as:

$$\tau_s(t) = B_0^{-1}(\theta)[\,a_1 \cdot \sigma(t) + (a_2 + b_0 + b_1|\theta| + b_2|\dot{\theta}|^2)sign(\sigma(t))] \quad (17)$$

where $(a_1, a_2) > 0$. The time derivative of the Lyapunov function becomes:

$$\begin{aligned}\dot{V}(t) &= \sigma(t)[-\alpha_2 \cdot k_2|e_2|^{\alpha_2-1} \cdot [B_o(\theta) \cdot \tau_s + \tau_{dis}]] \\ &= \sigma(t)[-\alpha_2 \cdot k_2|e_2|^{\alpha_2-1} \cdot [a_1 \cdot \sigma(t) + (a_2 + b_0 + b_1|\theta| + b_2|\dot{\theta}|^2)sign(\sigma(t)) + \tau_{dis}] \\ &= -\alpha_2 \cdot k_2|e_2|^{\alpha_2-1} \cdot [\,a_1 \cdot \sigma^2(t) + \left(a_2 + b_0 + b_1|\theta| + b_2|\dot{\theta}|^2\right)|\sigma(t)| + \sigma(t)\tau_{dis}]\end{aligned} \quad (18)$$

Using the assumption from Equation (6):

$$\dot{V}(t) \le \alpha_2 \cdot k_2|e_2|^{\alpha_2-1} \cdot [\,a_1\alpha^2(t) + a_2|\sigma(t)|\,] \quad (19)$$

Based on the Lyapunov theorem, using Equations (11) and (17), Convergence to the sliding surface is guaranteed$\sigma(t)$ and its maintenance on the surface. To demonstrate finite-time convergence, we consider the preceding analysis.

$$\dot{V}(t) \le -a_1\,\alpha_2 \cdot k_2|e_2|^{\alpha_2-1} \cdot \alpha^2(t) - a_2\alpha_2k_2|e_2|^{\alpha_2-1}|\sigma(t)|$$

$$\dot{V}(t) = \frac{dV(t)}{dt} \le -2 - a_1\,\alpha_2 \cdot k_2|e_2|^{\alpha_2-1}\,V(t) - \sqrt{2}\,\alpha^2(t) - a_2\alpha_2k_2|e_2|^{\alpha_2-1}\,V^{0.5}(t) \quad (20)$$

$$\frac{dV(t)}{dt} \le -\beta_1V(t) - \beta_2V^{0.5}(t)$$

Therefore, we can obtain:

$$dt \le \frac{-dV(t)}{\beta_1V(t) + \beta_2V^{0.5}(t)} = -2\,\frac{dV^{0.5}(t)}{\beta_1V^{0.5}(t) + \beta_2} \quad (21)$$

Let's define $t = t_c$ as the instant of system convergence to 0; integrating the above inequality and its simplification allows us to obtain:

$$t_c \le \frac{2}{\beta_1}\ln\left(\frac{\beta_1V^{0.5}(0) + \beta_2}{\beta_2}\right) \quad (22)$$

We can conclude that using the control law $\tau(t) = \tau_e + \tau_s$ (defined by their expressions in Equations (11) and (17) The closed-loop system is asymptotically stable with finite-time convergence to the desired trajectories. t_c. However, since this term τ_{dis} regroups unknown uncertainties and external disturbances,

calculating terms b_0, b_1 and b_2 is very difficult and complex. Furthermore, the term $F(\theta, \dot{\theta})$ can also contain uncertain terms like masses. To address this, we approximate them using four Type-2 Fuzzy Logic Systems (T2FLS) as follows:

$$\begin{aligned}\hat{F}(\theta,\dot{\theta}) &= \Lambda_F^T(t)\cdot\ \Phi_F(\ \theta,\ \dot{\theta}\ )\\ \hat{b}_0 &= \Lambda_0^T(t)\cdot\ \Phi_0(\ \theta,\ \dot{\theta}\ )\\ \hat{b}_1 &= \Lambda_1^T(t)\cdot\ \Phi_1(\ \theta,\dot{\theta}\ )\\ \hat{b}_2 &= \Lambda_2^T(t)\cdot\ \Phi_2(\ \theta,\dot{\theta})\end{aligned} \tag{23}$$

Per the universal approximation theorem, [4,28], there exists an optimal value of the interval type-2 fuzzy linguistic system (IT2FLS), which can be expressed as:

$$\begin{aligned}F(\theta,\dot{\theta}) &= \Lambda_F^T(t)\cdot\ \Phi_F^*(\theta,\dot{\theta})\\ b_0 &= \Lambda_0^T(t)\cdot\Phi_0^*(\theta,\dot{\theta})\\ b_1 &= \Lambda_1^T(t)\cdot\Phi_1^*(\theta,\dot{\theta})\\ b_2 &= \Lambda_2^T(t)\cdot\Phi_2^*(\theta,\dot{\theta})\end{aligned} \tag{24}$$

where $\Phi_F^*(\theta,\dot{\theta})$, $\Phi_0^*(\theta,\dot{\theta})$, $\Phi_1^*(\theta,\dot{\theta})$ and $\Phi_2^*(\theta,\dot{\theta})$ represent the optimal values of $\Phi_F(\theta,\dot{\theta}), \Phi_0(\theta,\dot{\theta}), \Phi_1(\theta,\dot{\theta})$ and $\Phi_2(\theta,\dot{\theta})$ respectively. Using Equation (23), the control becomes:

$$\tau(t) = \tau_e + \tau_s$$

$$\begin{aligned}\tau_e &= B_0^{-1}(t)[\ -\hat{F}(\theta,\dot{\theta}) + \ddot{\theta}_d +[\ \alpha_2\cdot k_2]^{-1}|e_2|^{2-\alpha_2}\text{sign}(e_2) +[\ \alpha_2\cdot k_2]^{-1}|e_2|^{2-\alpha_2}\ \alpha_1\cdot\\ &|e_1|^{\alpha_1-1}\text{sign}(e_2)\ ]\\ \tau_s &= B_0^{-1}(\theta)[\ a_1\sigma(t) + (a_2 + \widehat{b_0} + \widehat{b_1}|\theta| +\widehat{b_2}|\dot{\theta}|^2)\text{sign}(\sigma(t))]\end{aligned} \tag{25}$$

The ability of IT2FS to approximate any continuous function and the efficiency of sliding mode control to handle uncertainties allow the modified control laws in Equation (25) to ensure the same performances obtained in a classical case. To obtain the modification laws for the three adaptive fuzzy systems, we use apropos of the Lyapunov function:

$$V(t) = 0.5\sigma^2(t) + \frac{\alpha_2\cdot k_2}{2\gamma F}(\Phi_i^* - \Phi_i)^T(\Phi_F^* - \Phi_F) +\alpha_2 k_2 \sum_{i=0}^{3}(\Phi_i^* - \Phi_i)^T(\Phi_i^* - \Phi_i) \tag{26}$$

$$\begin{aligned}\dot{\Phi}_F &= \gamma F\sigma(t)|e_2|^{\alpha_2-1}\Lambda_F\\ \dot{\Phi}_0 &= \gamma_0|\sigma(t)||e_2|^{\alpha_2-1}\Lambda_0\\ \dot{\Phi}_1 &= \gamma_1|\sigma(t)||e_2|^{\alpha_2-1}|e_1|\Lambda_1\\ \dot{\Phi}_2 &= \gamma_2|\sigma(t)||e_2|^{\alpha_2}\Lambda_2\end{aligned} \tag{27}$$

Equation (26) It follows that the time derivative of the Lyapunov function can be written as:

$$\dot{V}(t) \leq\ \alpha_2\cdot k_2|e_2|^{\alpha_2-1}\ [\ -a_1\sigma^2(t) -\ a_2|\sigma(t)|\ ] \leq 0 \tag{28}$$

3. SIMULATION AND RESULTS

To evaluate the performance, a simulation of a SCARA robot, whose parameters are listed in Table 1, is conducted.

Table 1 Robot parameters and their value.

Axis	R_i	L_i	I_i	m_i
Axis 1 (Shoulder)	$0.25m$	$0.073m$	$0.065Kgm^2$	$6.32Kg$
Axis 2 (Elbow)	$0.25m$	$0.090m$	$0.056Kgm^2$	$5.51Kg$
Axis 3 (Wrist)	$0.25m$	$0.11m$	$0.011Kgm^2$	$1.37Kg$

To design the control laws in Equation (25), we must first construct the IT2FS:
$\hat{F}(\theta, \dot{\theta})$ is a 3X1 matrix whose parameters depend on both θ and $\dot{\theta}$. We note that θ and $\dot{\theta}$ are 3×1 vectors. To reduce the computation time, we propose to use 3IT2 fuzzy sets for each input $(\theta, \dot{\theta})$ in the form given in Figure 3. This structure of fuzzy sets is easy to implement with a reduced computing time.

The parameters $\hat{a}_0, \hat{a}_1 \, and \, \hat{a}_2$, are constructed by considering the sliding surface $\sigma(t)$ and for the derivative of time $\dot{\sigma}(t)$ as inputs, which allows to simplify the design procedure. computing time, we use IT2 fuzzy sets in the form given in (Figure 3) and we consider $\Lambda_0 = \Lambda_1 = \Lambda_2$. The initial values of the adjustable vectors Φ_i. Given by Equation (23) can be chosen equal to zero, or we can use the nominal model of our system to deduce these values as indicated in [21].

To test our controller, we consider parametric variations both in the masses m_i and lengths L_i, along with external disturbances. Figures 4 to 6 illustrate the tracking errors of the three joints for two different reference trajectories. We observe that these tracking errors converge to drive the state to zero within f or uncertainties and external disturbances, it will be a finite time, which meets the objectives of our approach. Furthermore, the shape of these curves makes it possible to confirm that the system's response is free from chattering.

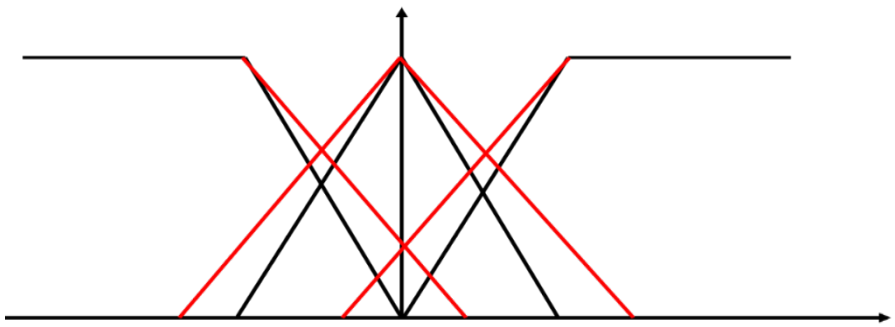

Figure 3 Triangular Type-2 fuzzy sets.

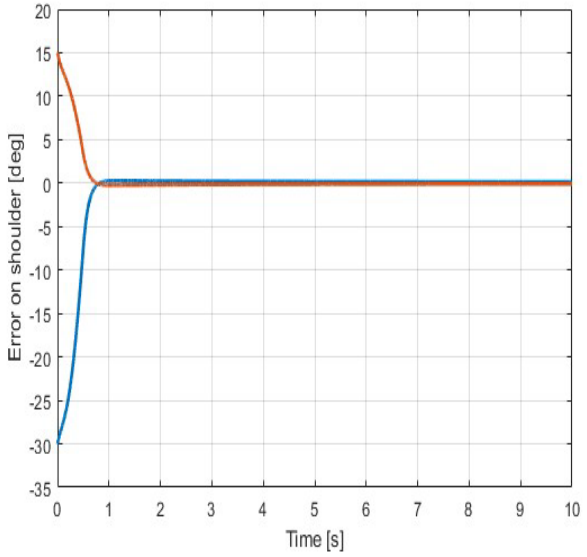

Figure 4 Tracking error on the shoulder joint.

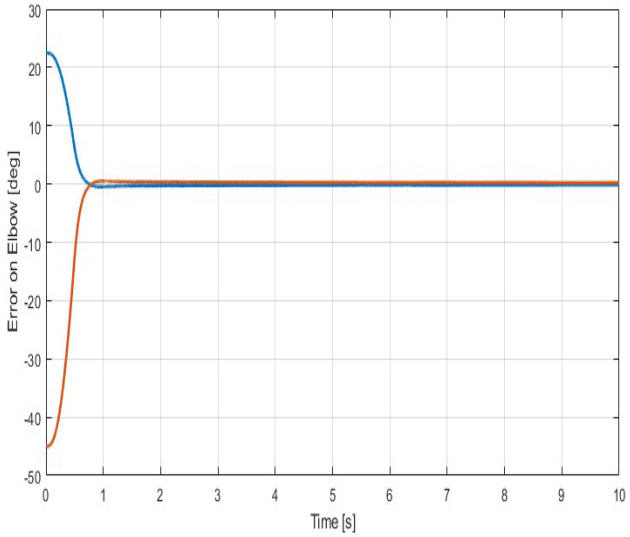

Figure 5 Tracking error on the elbow joint.

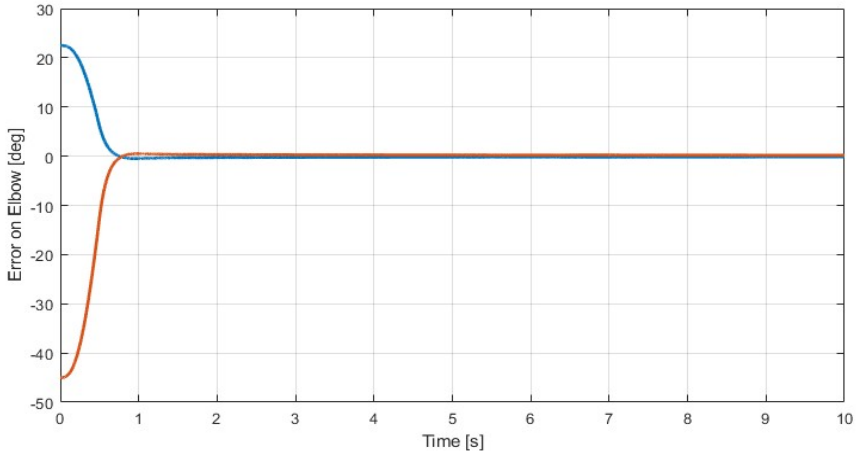

Figure 6 Tracking error on the wrist joint.

4. CONCLUSIONS

In this work, we combine the performance of a fast-modelling control with the capabilities of interval type-2 fuzzy logic to design a control for a robot. Demonstrated, for the closed-loop system with this control, by the theoretical claims and the results are provided to support. Despite these positive results, we aim to further enhance the implementation by using bio-inspired algorithms to optimize the parameters.

APPENDIX A

Dynamical Model of SCARA Robot
The expression of the used matrices in the dynamical model of the SCARA robot (1).

$$M = \begin{bmatrix} M_{11} & M_{12} & M_{13} \\ M_{21} & M_{22} & M_{23} \\ M_{31} & M_{32} & M_{33} \end{bmatrix} \quad V = \begin{bmatrix} V_{11} & V_{12} & V_{13} \\ V_{21} & V_{22} & V_{23} \\ V_{31} & V_{32} & V_{33} \end{bmatrix}$$

$$M_{11} = (I_1 + I_2 + I_3) + m_1 L_1^2 + m_2(L_2^2 + R_1^2 - 2L_2 R_1 \cos(\theta_E) + m_3(L_3^2 + R_2^2 + R_1^2 - 2L_3 R_2 \cos(\theta_W) + 2L_3 R_1 \cos(\theta_E + \theta_W) - 2R_1 R_2 \cos(\theta_E))$$

$$M_{12} = (I_2 + I_3) + m_2(L_2^2 - L_2 R_1 \cos(\theta_E) + m_3(L_3^2 + R_2^2 + 2L_3 R_2 \cos(\theta_E) + m_3(L_3^2 + R_2^2 + 2L_3 R_2 \cos(\theta_E) + L_3 R_1 \cos(\theta_E + \theta_W) - R_2 R_1 \cos(\theta_E))$$
$$M_{13} = I_3 + m_2(L_2^2 + L_3 R_2 \cos(\theta_W)) + L_3 R_1 \cos(\theta_E + \theta_W))$$

$$M_{21} = (I_2 + I_3) + m_2(L_2^2 + L_2 R_1 \cos(\theta_E)) - m_3(L_3^2 + R_2^2 + 2L_3 R_2 \cos(\theta_W)) + L_3 R_1 \cos(\theta_E + \theta_W) + R_1 R_2 \cos(\theta_E))$$

$$M_{22} = (I_2 + I_3) + m_2 L_2^2 + m_3(L_3^2 + R_2^2 + 2L_3 R_2 \cos(\theta_W))$$

$$M_{23} = I_3 + m_3(L_3^2 + L_3 R_2 \cos(\theta_W))$$

$$M_{31} = I_3 + m_3 L_3^2 + m_3 L_3 R_2 \cos(\theta_W)) + m_3 L_3 R_1 \cos(\theta_E + \theta_W))$$

$$M_{32} = I_3 + m_3 L_3^2 + m_3 L_3 R_2 \cos(\theta_W))$$

$$M_{33} = I_3 + m_3 L_3^2$$

$$V_{11} = (2L_3 R_1 m_3 \sin(\theta_E + \theta_W) + 2L_2 R_1 m_2 \sin(\theta_E) + 2R_1 R_2 m_3 \sin(\theta_E))\dot{\theta}_E - (2L_3 R_1 m_3 \sin(\theta_E + \theta_W) + 2L_3 R_2 m_3 \sin(\theta_W))\dot{\theta}_W$$

$$V_{12} = (-L_3 R_1 m_3 \sin(\theta_E + \theta_W) - 2L_2 R_1 m_2 \sin(\theta_E) - 2R_1 R_2 m_3 \sin(\theta_E))\dot{\theta}_E$$

$$V_{13} = (-2L_3 R_1 m_3 \sin(\theta_E + \theta_W) - 2L_3 R_2 m_3 \sin(\theta_E))\dot{\theta}_E - L_3 R_1 m_3 \sin(\theta_E + \theta_W) + L_3 R_2 m_3 \sin(\theta_W)\dot{\theta}_W$$

$$V_{21} = (L_3 R_1 m_3 \sin(\theta_E + \theta_W) + L_2 R_1 m_2 \sin(\theta_E) + R_1 R_2 m_3 \sin(\theta_E))\dot{\theta}_S$$

$$V_{22} = -2L_3 R_2 m_3 \sin(\theta_W)\theta_W$$

$$V_{23} = -2L_3 R_2 m_3 \sin(\theta_W)\dot{\theta}_S - L_3 R_2 m_3 \sin(\theta_W)\dot{\theta}_W$$

$$V_{31} = (L_3 R_1 m_3 \sin(\theta_W + \theta_W) + L_3 R_2 m_3 \sin(\theta_W)\dot{\theta}_S$$

$$V_{32} = 2L_3 R_2 m_3 \sin(\theta_W)\dot{\theta}_S + L_3 R_2 m_3 \sin(\theta_W)\dot{\theta}_E$$
$$V_{33} = 0$$

References

[1] Z. K. Salih, A. A. Kamall-Eldeen, Exp. Theor. Nanotechnol. 8 (2024) 27 doi:10.56053/8.2.27
[2] K. D. Young, V. I. Utkin, U. Ozguner, IEEE Trans. Control Syst. Technol. 7 (1999) 328 doi:10.1109/87.761053
[3] Ya-Chen Hsu, Guanrong Chen, Han-Xiong Li, IEEE Trans. Syst. Man Cybern. Part B Cybern. 31 (2001) 331 doi:10.1109/3477.931517
[4] L. Alnufaie, Int. J. Adv. Eng. Res. Sci. 10 (2023) 78 doi:10.22161/ijaers.1011.9
[5] N. Essounbouli, A. Hamzaoui, J. Zaytoon, IFAC Proc. 35 (2002) 157 doi:10.3182/20020721-6-ES-1901.00679
[6] F. Du, Sun Ying, Li Gongfa, Jiang Guozhang, Int. J. Wirel. Mob. Comput. 13 (2017) 306 doi:10.1504/IJWMC.2017.089324
[7] L. Zhan, K. Zhou, Int. J. Adv. Manuf. Technol. 69 (2013) 1469 doi:10.1007/s00170-013-5123-6
[8] M.-D. Duong, Q.-T. Pham, T.-C. Vu, N.-T. BUI, Q.-T. Dao, Sci. Rep. 13 (2023) 8242 doi:10.1038/s41598-023-34491-3
[9] A. Abbasimoshaei, M. Mohammadimoghaddam, T. A. Kern, in Haptics: Science, Technology, Applications, 12272 (2020) 506 doi:10.1007/978-3-030-58147-3_56
[10] L. A. Nufaie, Int. J. Adv. Res. 11 (2023) 343 doi:10.21474/IJAR01/17397
[11] S.-H. Han, M. S. Tran, D.-T. Tran, Appl. Sci. 11 (2021) 3919 doi:10.3390/app11093919
[12] X. Chen, Automatica, 42 (2006) 427 doi:10.1016/j.automatica.2005.10.008
[13] J. Fei, H. Ding, Nonlinear Dyn. 70 (2012) 1563 doi:10.1007/s11071-012-0556-2
[14] Y.-J. Huang, T.-C. Kuo, S.-H. Chang, IEEE Trans. Syst. Man Cybern. Part B Cybern. 38 (2008) 534 doi:10.1109/TSMCB.2007.910740
[15] J.-H. Hwang, Y.-C. Kang, J.-W. Park, D. W. Kim, Comput. Intell. Neurosci. 2017 (2017) 1 doi:10.1155/2017/9640849
[16] Badis Bendjemil, Maram Mechi, Khaoula Safi, Mounir Ferhi, Karima Horchani Naifer, Exp. Theo. NANOTECHNOLOGY 8 (2024) 51 https://doi.org/10.56053/8.3.51
[17] M. Sugeno, Inf. Sci. 36 (1985) 59 doi:10.1016/0020-0255(85)90026-X
[18] F. Piltan, A. Nabaee, M. Ebrahimi, M. Bazregar, Int. J. Inf. Technol. Comput. Sci. 5 (2013) 123 doi: 10.5815/ijitcs.2013.08.12
[19] S. Amirkhani, S. Mobayen, N. Iliaee, O. Boubaker, S. H. Hosseinnia, Int. J. Adv. Robot. Syst. 16 (2019) 1729 doi:10.1177/1729881419828176
[20] M. Van, S. S. Ge, H. Ren, IEEE Trans. Cybern. 47 (2017) 1681 doi:10.1109/TCYB.2016.2555307
[21] C. C. Lee, IEEE Trans. Syst. Man Cybern. 20 (1990) 404 doi:10.1109/21.52551
[22] L. Alnufaie, Int. J. Adv. Appl. Sci. 10 (2023) 166 doi:10.21833/ijaas.2023.10.019
[23] A. M. Ahmed Alwaise, Raqeeb H. Rajab, Adel A. Mahmood, Mohammed A. Alreshedi, Exp. Theo. NANOTECHNOLOGY 8 (2024) 67 https://doi.org/10.56053/8.3.67
[24] M. Manceur, N. Essounbouli, A. Hamzaoui, IEEE Trans. Fuzzy Syst. 20 (2012) 262 doi:10.1109/TFUZZ.2011.2172948
[25] S. M. Fathi, N. A. Al-Kareem, Exp. Theo. NANOTECHNOLOGY 9 (2025) 199 https://doi.org/10.56053/9.S.199
[26] B. Reetz, A. Frehn, W. Budweiser, W. Bishop, Exp. Theo. NANOTECHNOLOGY 9 (2025) 465 https://doi.org/10.56053/9.3.465
[27] N. Nafia, A. El Kari, H. Ayad, M. Mjahed, Robotics 7 (2018) 40 doi:10.3390/robotics7030040
[28] N. Kim, Park Yunki, Son Jung E., Shin Seongjin, Min Byounghyuk, Park Hyungjin, Int. J. Control Autom. Syst. 16 (2018) 62 doi:10.1007/s12555-016-0584-7